

# Interdomain Communication in Hepatitis C Virus Polymerase Abolished by Small Molecule Inhibitors Bound to a Novel Allosteric Site\*<sup>§</sup>

Received for publication, May 17, 2005

Published, JBC Papers in Press, June 13, 2005, DOI 10.1074/jbc.M505423200

Stefania Di Marco<sup>‡</sup>, Cinzia Volpari, Licia Tomei, Sergio Altamura, Steven Harper, Frank Narjes, Uwe Koch, Michael Rowley, Raffaele De Francesco, Giovanni Migliaccio, and Andrea Carfi<sup>§</sup>

From the Istituto di Ricerche di Biologia Molecolare P. Angeletti, 00040 Pomezia (Rome), Italy

**The hepatitis C virus (HCV) polymerase is required for replication of the viral genome and is a key target for therapeutic intervention against HCV. We have determined the crystal structures of the HCV polymerase complexed with two indole-based allosteric inhibitors at 2.3- and 2.4-Å resolution. The structures show that these inhibitors bind to a site on the surface of the thumb domain. A cyclohexyl and phenyl ring substituents, bridged by an indole moiety, fill two closely spaced pockets, whereas a carboxylate substituent forms a salt bridge with an exposed arginine side chain. Interestingly, in the apoenzyme, the inhibitor binding site is occupied by a small  $\alpha$ -helix at the tip of the N-terminal loop that connects the fingers and thumb domains. Thus, these molecules inhibit the enzyme by preventing formation of intramolecular contacts between these two domains and consequently precluding their coordinated movements during RNA synthesis. Our structures identify a novel mechanism by which a new class of allosteric inhibitors inhibits the HCV polymerase and open the way to the development of novel antiviral agents against this clinically relevant human pathogen.**

The hepatitis C virus (HCV)<sup>1</sup> is a small positive-strand RNA virus responsible for a considerable proportion of acute and chronic hepatitis in humans (1, 2). It is estimated that more than 170 million people worldwide are infected by this virus (3). There is no vaccine available for HCV, and the current therapy, based on interferon and ribavirin, is poorly tolerated and of limited efficacy. Therefore, there are intense research efforts toward the development of new drugs targeting essential HCV

enzymes and in particular the polymerase. The HCV nonstructural protein 5B (NS5B) is the RNA-dependent RNA polymerase (RdRp) responsible for replication of the viral genome. NS5B can initiate RNA synthesis by two different mechanisms: primer-independent initiation from the 3' terminus of the viral genome, also known as *de novo* initiation (4, 5), and primer-dependent initiation using either DNA or RNA as primers (6). The *de novo* synthesis is likely used during virus replication in infected cells (7).

The three-dimensional structures of soluble forms of the HCV polymerase genotype 1b,  $\Delta$ C21 and  $\Delta$ C55, lacking the last 21 and 55 C-terminal residues, respectively, have been reported (8–10). These structures revealed a classical “right hand” shape formed by the palm, thumb, and fingers domains as initially defined in the Klenow fragment of *Escherichia coli* DNA polymerase I (11) and showed the presence of an extension in the fingers, the so-called fingertip subdomain, containing two loops,  $\Lambda$ 1 and  $\Lambda$ 2 (secondary structure nomenclature according to Ref. 9), which anchor the fingers to the thumb. As a result, the polymerase has a relatively closed and spherical appearance, and the active site cavity, to which the RNA template and the NTP substrates have access via two positively charged tunnels, is completely encircled. Structural studies have shown that other viral RdRps, such as those of poliovirus (12, 13), human rhinovirus (14, 15), bovine viral diarrhea virus (16), rabbit hemorrhagic disease virus (17), reovirus (18), and bacteriophage  $\phi$ 6 (19), have the same global architecture and a similar closed conformation. Crystal structures of NS5B bound to a short RNA template or to NTPs have also been solved (20, 21). Interestingly, in all these structures, ligand binding occurred without rearrangements in the enzyme domains. Moreover, the structure of the NS5B-GTP complex showed that, in addition to the active site, GTP can also bind to an exposed site on the thumb domain in close proximity to the tip of the fingertip  $\Lambda$ 1 loop (21). This external GTP site, 30 Å away from the polymerase catalytic center, was proposed to exert a regulatory activity by modulating the interactions between the fingers and thumb domains during RNA synthesis. Recently, the structure of the HCV polymerase genotype 2a (this enzyme shares 70% sequence identity with the 1b polymerase) was reported (22). This study revealed two conformations of the enzyme: closed, similar to the apo1b polymerase structure, and a more opened structure. Interestingly, in the opened conformation the tip of the fingertip  $\Lambda$ 1 loop, which is  $\alpha$ -helical in the closed conformation of the polymerase, moved away from the thumb domain and adopted a  $\beta$ -hairpin-like structure.

The discovery and characterization of a number of structurally diverse non-nucleoside inhibitors (NNIs) of the HCV polymerase have been reported (22–26). These molecules inhibited the polymerase at a stage preceding the elongation step and

\* This work was supported by a grant from the Ministero dell'Istruzione, dell'Università e della Ricerca. The costs of publication of this article were defrayed in part by the payment of page charges. This article must therefore be hereby marked “advertisement” in accordance with 18 U.S.C. Section 1734 solely to indicate this fact.

<sup>§</sup> The on-line version of this article (available at <http://www.jbc.org>) contains supplemental Fig. 6 and supplemental Table II.

The atomic coordinates and structure factors (code 2BRK and 2BRL) have been deposited in the Protein Data Bank, Research Collaboratory for Structural Bioinformatics, Rutgers University, New Brunswick, NJ (<http://www.rcsb.org/>).

<sup>‡</sup> To whom correspondence may be addressed: Istituto di Ricerche di Biologia Molecolare P. Angeletti, Via Pontina Km 30.600, 00040 Pomezia, Rome, Italy. Tel.: 39-06-91093238; Fax: 39-06-91093654; E-mail: stefania\_dimarco@merck.com.

<sup>§</sup> To whom correspondence may be addressed: Istituto di Ricerche di Biologia Molecolare P. Angeletti, Via Pontina Km 30.600, 00040 Pomezia, Rome, Italy. Tel.: 39-06-91093550; Fax: 39-06-91093654; E-mail: andrea\_carfi@merck.com.

<sup>1</sup> The abbreviations used are: HCV, hepatitis C virus; RdRp, RNA-dependent RNA polymerase; NNI, non-nucleoside inhibitor; DTT, dithiothreitol; MES, 2-morpholinoethanesulfonic acid.

non-competitively with RNA template or NTPs (24, 25). Despite these common features in the mechanism of inhibition, structural, genetic, and biochemical evidence suggest that HCV NNIs bind to different sites on the polymerase. Specifically, crystallographic studies indicate that inhibitors based on thio-phenone, phenylalanine, or dihydropyranone scaffolds bind in a hydrophobic cleft in the thumb domain near the C terminus of the polymerase and 10–15 Å from the external GTP site (21–23). Conversely, a combination of genetic and biochemical data suggests that a second group of NNIs, comprising compounds based on the structurally related benzimidazole and indole core, binds at the exposed GTP site (24, 25). In agreement with this hypothesis, resistance to these inhibitors arises through mutation of Pro-495, a residue involved in the interaction with the external GTP molecule, and enzyme binding and inhibition are antagonized by GTP (24). Benzimidazole- and indole-derived NNIs have provided encouraging results as anti-HCV agents. In a recent study indole-based inhibitors were shown to be devoid of off-target activities and presented encouraging pharmacokinetic profiles in preclinical animal studies (27). In addition, a benzimidazole polymerase inhibitor has entered into Phase I/II clinical trials (28).

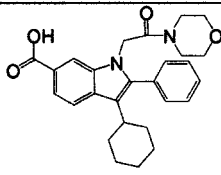
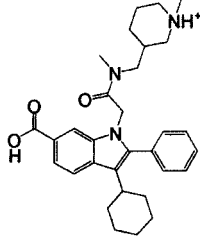
Here we describe the crystal structures of the HCV polymerase in complex with two indole-derived NNIs. These structures reveal a novel inhibitory binding site in the polymerase and open the way to the design of new NNIs for treatment of HCV infection. Furthermore, our structures suggest a mechanism of inhibition, with the inhibitor displacing part of the fingertip loop anchoring the fingers domain to the thumb domain, which may also be relevant for the inhibition of other viral RdRps.

#### MATERIALS AND METHODS

**Protein Expression and Purification**—A variant of HCV NS5B (genotype 1b, strain BK) lacking 55 C-terminal residues ( $\Delta$ C55) and a P495L point mutant (24) have been expressed and purified as detailed below. Protein overexpression was performed by induction of mid-log phase BL21 DE3 *E. coli* cells with 0.4 mM isopropyl-1-thio- $\beta$ -D-galactopyranoside for 22 h at 18 °C in LB medium. Harvested bacteria were resuspended in ice-cold lysis buffer (20 mM Tris-HCl, pH 7.5, 300 mM NaCl, 20% glycerol, 0.2%  $\beta$ -octylglucoside, 1 mM EDTA, 10 mM dithiothreitol (DTT), and Complete™ EDTA-free protease inhibitor mixture tablets) and lysed with a cell disruptor (Costant System). Lysate was incubated with DNase I (5 units/ml) in the presence of 10 mM MgCl<sub>2</sub> and clarified by centrifugation at 35,000  $\times g$  for 1 h. The supernatant was loaded onto a heparin column pre-equilibrated with buffer A-Hep (20 mM Tris-HCl, pH 7.5, 300 mM NaCl, 20% glycerol, 0.2%  $\beta$ -octylglucoside, 1 mM EDTA, 10 mM DTT) at 4 °C, and the protein was eluted with a salt gradient in 700 mM NaCl. Protein fractions were pooled and diluted with the A-Hep buffer without NaCl to reach 150 mM NaCl and loaded onto an ion-exchange Resource S column pre-equilibrated in A-S buffer (20 mM Tris-HCl, pH 7.5, 150 mM NaCl, 20% glycerol, 0.2%  $\beta$ -octylglucoside, 1 mM EDTA, and 10 mM DTT). The column was washed in buffer with 300 mM NaCl, and the protein was subjected to a linear gradient from 300 mM to 1 M NaCl. The protein elutes at ~500 mM NaCl. Fractions were loaded onto a Sephadex G75 gel filtration column equilibrated in 20 mM Tris-HCl, pH 7.5, 500 mM NaCl, 20% glycerol, 0.2%  $\beta$ -octylglucoside, 1 mM EDTA, and 10 mM DTT. The protein was analyzed by electrospray ionization-mass spectrometry and confirmed to be >95% pure, with an experimental mass of 59,555 Da (theoretical mass 59,561 Da). The full-length NS5B protein and the  $\Delta$ C21 protein, a NS5B variant with the last 21 C-terminal residues deleted, were expressed and purified as described previously (29, 30). Details of the polymerase activity assay and replicon analysis have been described in Ref. 24.

**Crystallization and Data Collection**—NS5B- $\Delta$ C55 crystals were grown as described previously (9). Inhibitor soakings were performed by transferring crystals in a solution containing 100 mM MES, pH 6.0, 14% polyethylene glycol 8,000, 14% 2-propanol, 10 mM DTT, 10 mM MnCl<sub>2</sub>, and 2.5 mM of compound 1 or 2. Soaking was performed for only 20–30 min as crystals had the tendency to crack ~40–60 min after inhibitor addition. Crystals were then transferred for 1 min to a cryoprotectant solution containing 100 mM MES, pH 6.0, 14% polyethylene glycol 8,000, 14% 2-propanol, 18% 2-methyl-2,5-pentanediol, 10 mM DTT, 5

TABLE I  
Potency of compounds 1 and 2

Compound	IC <sub>50</sub> (nM)		
	$\Delta$ C55	$\Delta$ C55 P495L	Replicon
 1*	26	N.A. <sup>†</sup>	800
 2	18	N.A.	300

\* Compound 1, 3-cyclohexyl-1-(2-morpholin-4-yl-2-oxoethyl)-2-phenyl-1H-indole-6-carboxylic acid; compound 2, 3-cyclohexyl-1-(2-[methyl[(1-methylpiperidin-3-yl)methyl]amino]-2-oxoethyl)-2-phenyl-1H-indole-6-carboxylic acid.

<sup>†</sup> N.A., not active up to 10  $\mu$ M.

mM MnCl<sub>2</sub>, and 1.25 mM compound 1 or 2. Diffraction data were collected at 100 K from cryo-cooled crystals at the ID14-H1 beam-line at the European Synchrotron Radiation Facility (Grenoble, France). Data were processed with MOSFLM and scaled with SCALA (31). Data collection statistics are summarized in supplemental Table II. Further data processing and analysis were performed with the CCP4 suite of programs (31).

**Structure Determination and Refinement**—Crystals of the apoprotein grew in space group P2<sub>1</sub>2<sub>1</sub>2<sub>1</sub>, with two molecules in the asymmetric unit (9), but after soaking, the space group shifted to P2<sub>1</sub>2<sub>1</sub>2<sub>1</sub> with one molecule in the asymmetric unit (supplemental Table II), similar to what was described for the structure of the polymerase-GTP complex (21). The two structures of the  $\Delta$ C55 polymerase-inhibitor complexes were solved by the molecular replacement method with the program AMoRe from CCP4 (31) using the structure of the apo $\Delta$ C55 as a search model (9). Model building with QUANTA (Accelrys, San Diego, CA) and refinement with REFMAC from CCP4 (31), using a maximum likelihood target, resulted in the final models (supplemental Table II). No electron density was present for residues 22–35, 148–152, and 532–536, which were therefore excluded from the refinement. Both structures satisfy all the criteria set by the program PROCHECK (32), and all amino acids lie in allowed regions of the Ramachandran plot.

#### RESULTS AND DISCUSSION

**Inhibition of HCV Polymerase**—The key pharmacophore elements of the allosteric inhibitors used in this study include a central scaffold of a 6,5-fused ring system, which proved to be optimal (27), an acid, a cyclohexyl and an aryl substituent (Table I). The only difference between the two inhibitors resides in the indole *N*-acetyl substituent. Both compounds inhibited the purified enzyme with IC<sub>50</sub> values in the low nM range and subgenomic HCV RNA replication in the sub- $\mu$ M range (Table I). Inhibition was independent of the form of recombinant polymerase used as both full-length and C-terminally truncated  $\Delta$ C21 and  $\Delta$ C55 were inhibited with similar IC<sub>50</sub> values (for compound 2 the IC<sub>50</sub> values for the full-length and  $\Delta$ C21 enzymes were 22 and 100 nM, respectively).

**Inhibitor Binding and Polymerase Conformational Change**—The crystal structures of the  $\Delta$ C55 polymerase in complex with compound 1 (2.3-Å resolution) and compound 2 (2.4-Å resolution) were obtained by soaking procedures. In both cases, anal-

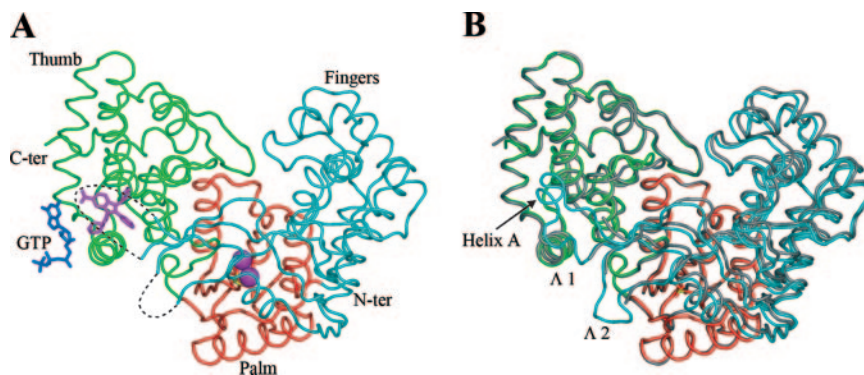


FIG. 1. **Conformational changes in HCV NS5B associated with inhibitor binding.** *A*, ribbon diagram of the inhibited structure. Fingers, palm, and thumb domains are colored cyan, red, and green, respectively. The inhibitor (compound 1) is shown in stick representation and colored magenta. The GTP molecule (dark blue), as revealed by previous structural work (21), and two  $Mn^{2+}$  ions (magenta spheres) in the catalytic site are also shown. The metal ions are coordinated by Asp-220, Asp-318, Asp-319, and several water molecules, but only Asp-220 is shown. Disordered regions are shown as dashed black lines. *C-ter*, C terminus; *N-ter*, N terminus. *B*, the  $\Delta C55$  apostructure (9) (colored as in *A*) superimposed on the inhibited structure (gray). Figs. 1–3 were generated with PyMOL (DeLano Scientific).

ysis of the initial electron density map showed clearly defined electron density for the inhibitor (supplemental Fig. 6). However, different from what was predicted (24), binding did not occur at the exposed GTP binding site but instead 8 Å from it in a site occupied in the apoenzyme by the small  $\alpha$ -helix A at the tip of the fingertip  $\Lambda 1$  loop (Fig. 1). This loop anchors the fingers to the thumb in the apoenzyme and opens in the direction of the solvent, becoming partially disordered in the inhibitor-bound structures with no electron density present for residues 22–35 (Fig. 1). Electron density was also missing for residues 148–152, part of the fingertip  $\Lambda 2$  loop that is adjacent to the  $\Lambda 1$  loop and also connects the fingers and thumb (Fig. 1). This region is already flexible in the  $\Delta C55$  apostructure (9) but is completely disordered in the inhibited structures, presumably because of the lack of stabilization provided in the apoenzyme by the interaction between  $\Lambda 2$  Val-147 and  $\Lambda 1$  Met-36. Another consequence of the displacement of  $\alpha$ -helix A and the resulting weaker interaction between the thumb and fingers is a slight opening of the polymerase. Indeed, when the palm and thumb domains of the inhibited structure and the apostructure are superimposed, we observed a rigid body rotation of the fingers of 2–4° in a clockwise direction with respect to the palm. Furthermore, the differences in  $C\alpha$  positions in the fingers domain varied between 0.5 and 2.1 Å (Fig. 1B). It cannot be excluded that the rearrangement of the polymerase domains may have been limited in the crystals by packing interactions and thus could be even larger in solution. Indeed, crystals could be soaked in the presence of the inhibitor only for a relatively short amount of time. An opening of the polymerase, following inhibitor binding, might prevent either the correct positioning of RNA and NTPs required for catalysis or the translocation of the template and product.

**Inhibitor-Enzyme Interactions**—Despite having a different indole *N*-acetyl substituent (Table I) the two inhibitors bind almost identically to the polymerase (Fig. 2A). In fact only two carbon atoms of the *N*-acetyl substituent are in van der Waals contact distance with the backbone carbonyl oxygen atoms of Leu-492 and Gly-493 (Fig. 2B), explaining the similar binding modes and  $IC_{50}$  values for the two molecules (Table I).

The inhibitor-polymerase interaction is mainly hydrophobic. The only exception is a salt bridge formed by the carboxylate group of the inhibitor and the guanidinium group of Arg-503. Plausibly, Arg-503 and the proximal His-428 side chains create a positive electrostatic potential favorable for the binding of acidic ligands (Fig. 2B). The cyclohexyl and the phenyl ring substituents likely contribute to most of the binding energy by filling two closely spaced pockets of the binding site. The side

chains of Leu-392, Ala-395, Thr-399, Ile-424, Leu-425, His-428, and Phe-429 form a deep pocket, filled almost completely by the cyclohexyl group of the inhibitor, whereas the Val-37, Leu-392, Ala-393, Ala-396, Leu-492, and Val-494 side chains form a narrower pocket occupied by the inhibitor phenyl ring (Fig. 2B). Interestingly, none of these residues changed conformation compared with the apostructure. The indole core bridges the two groups and also contributes both in filling the pockets and in the interaction with the protein. One side of the indole moiety points toward the pocket interior and interacts with the Val-494 and Trp-500 side chains, whereas the other side makes van der Waals contacts with the exposed Pro-495 pyrrol ring on the external lower side of the pocket (Fig. 2B). The latter interaction likely explains the lack of inhibition by this class of compounds of the NS5B P495L point mutant (Table I) (24).

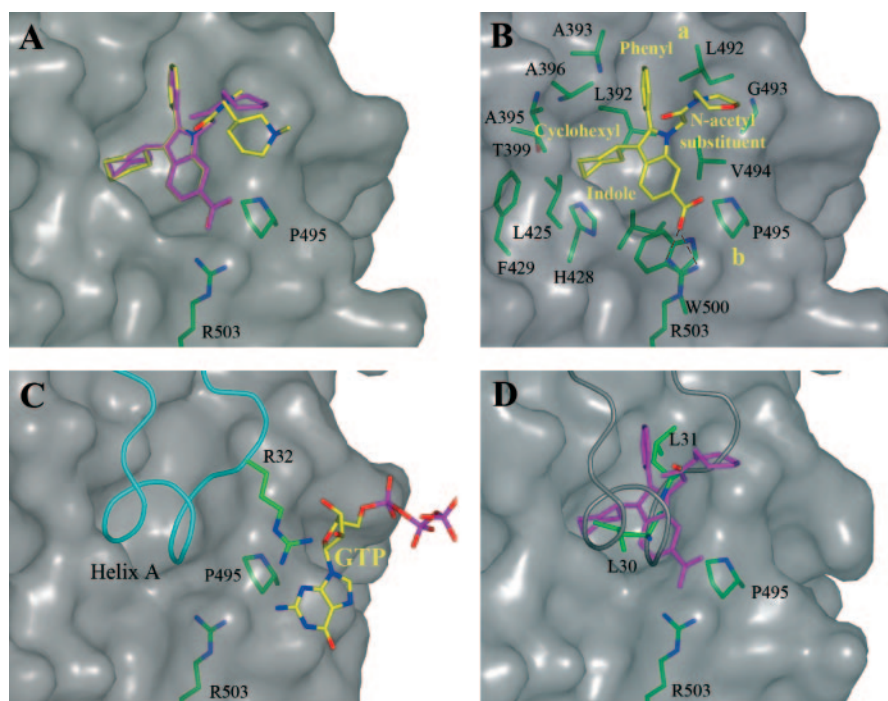
The structures suggest several ways to improve the potency of this class of inhibitors (Fig. 2B). In the direction perpendicular to the plane of the indole moiety the occupancy of the pocket is not complete, and slightly bulkier moieties may increase the contact area by approaching Val-494. Substituents inserted at the para-position of the phenyl ring could extend into a protein hydrophobic cleft (designated as “a” in Fig. 2B), significantly increasing the surface contact area. The *N*-acetamide substituent could be modified to form hydrogen bonds with the backbone oxygens of Leu-492 and Gly-493. Finally, a larger group could substitute for one of the carboxylate oxygens, so as to extend the inhibitor into a second hydrophobic region (designated as “b” in Fig. 2B), while keeping with the other oxygen the polar interaction with the side chain of Arg-503 (Fig. 2, A and B). In agreement with this hypothesis, a structurally related indole-scaffolded inhibitor, containing the same cyclohexyl and phenyl substituents and an additional elongated amide extension in this position, inhibits the NS5B polymerase with a subnanomolar  $IC_{50}$ .<sup>2</sup>

**Indole-based NNIs and Other Small Molecule Binding Sites**—Comparison of the NS5B-GTP complex structure (21) with our structures shows that the binding sites for GTP and for the indole-based inhibitors are close in space but clearly distinct. The GTP molecule lies on a shallow surface in proximity to the fingertip  $\alpha$ -helix A, whereas the inhibitor fills the pocket occupied in the apoenzyme by the same  $\alpha$ -helix (Fig. 2, A and C). Moreover, GTP binding is not associated with any

<sup>2</sup> S. Harper, unpublished data.



**FIG. 2. Inhibitor binding site in the thumb domain.** This view is obtained after a roughly 180° clockwise rotation of the view shown in Fig. 1A. Protein residues are drawn in *stick representation*. Red, oxygen; blue, nitrogen; green, carbon. **A**, superposition of the crystal structures with compounds 1 (magenta) and 2 (atom color coding: red, oxygen; blue, nitrogen; yellow, carbon). **B**, residues involved in inhibitor binding and compound 1 (color coding for atoms as described in A). Val-37 from the fingers domain also makes hydrophobic interaction with the inhibitor phenyl ring but is not shown here. Polar interactions are shown as *dashed black lines*. Yellow letters *a* and *b* indicate regions that might be explored for the generation of more potent compounds. **C**, GTP binding site in the thumb domain as revealed by Ref. 21. The color coding for the GTP molecule atoms is: red, oxygen; blue, nitrogen; yellow, carbon; magenta, phosphate. Main chains for residues 18–36 from the fingers are shown as a *cyan coil*. **D**, superposition of the apo $\Delta$ C55 structure (9) with the inhibited structure (compound 1). The main chain backbone atoms for residues 18–36 are shown as a *gray coil*. Leu-30 (L30) and Leu-31 (L31) (green) from  $\alpha$ -helix A and compound 1 (magenta) are also shown.



protein conformational change (21), whereas inhibitor binding requires a displacement of the  $\alpha$ -helix A and part of the  $\Lambda$ 1 loop (Fig. 2, C and D). However, GTP and inhibitors make some common interactions with polymerase atoms (Fig. 2, B and C). Both molecules are at van der Waals contact distances with Pro-495, although they lie on opposite sides of the pyrrol ring. Further, both molecules interact with the Arg-503 side chain; the GTP molecule establishes one water-mediated hydrogen bond, whereas the inhibitor forms a salt bridge via its carboxylate group (Fig. 2, B and C). Interestingly, in the NS5B-GTP complex the ribose moiety of GTP hydrogen bonds the guanidinium group of Arg-32 (Fig. 2C). This interaction may contribute to tightening the association of the fingertip  $\Lambda$ 1 loop with the thumb and could disfavor the opening of the loop and consequently the access of the inhibitor to its binding site. Together, the interaction with common residues and between Arg-32 and GTP provides an explanation for the antagonistic effect that high concentrations of GTP have on polymerase inhibition by this class of compounds (24).

The binding site for the indole-based inhibitors is also distinct from the binding site for another group of NNIs based on thiophene, phenylalanine, or dihydropyranone scaffolds. These compounds bind to a common site on an elongated hydrophobic cleft in the thumb domain near the C terminus of the polymerase (Fig. 3A) (21–23, 26). Although the binding sites for this group of compounds and for the indole-based inhibitors are 14 Å apart, they reside on opposite sides of the thumb domain helix Q, which in turn contacts helices S and T (Fig. 3B). Thus, it is conceivable that these two distinct inhibitor binding sites are functionally linked through these secondary structural elements. This hypothesis is supported by recent structures of the 2a polymerase alone and bound to two thiophene-based NNIs (22). In this study the tip of the 2a polymerase  $\Lambda$ 1 loop was shown to adopt two different conformations, helical and  $\beta$ -hairpin-like. The  $\alpha$ -helical conformation was associated with a closed polymerase structure similar to the 1b apostructure, whereas in the  $\beta$ -hairpin-like conformation the polymerase adopted a more opened structure (22). Interestingly, the inhibitors could bind only to the closed form of the enzyme and induced a transition to the opened conformation. Thus, al-

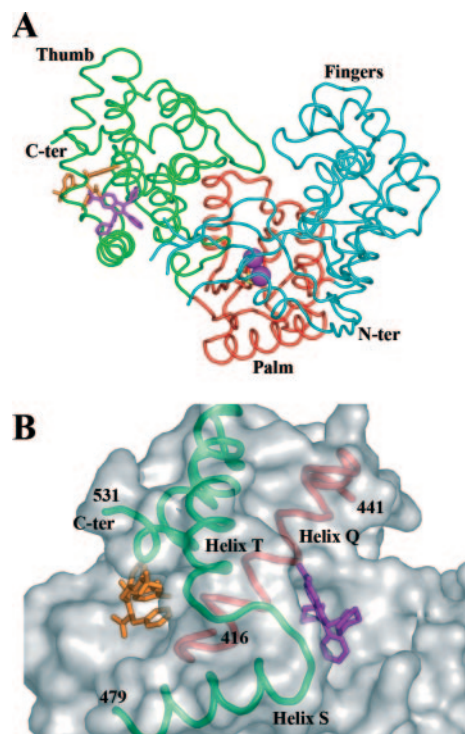


**FIG. 3. Two allosteric inhibitor binding sites in the thumb domain.** **A**, ribbon diagram of our inhibited structure with compound 1 (magenta stick) superimposed to the 1b polymerase structure bound to phenylalanine-based inhibitor (26). For this structure only the inhibitor is shown (orange stick). The color coding is as in Fig. 1A. **B**, close-up view of the thumb domain with secondary structural elements, helices Q, S, and T, close to the two inhibitor binding sites (compound 1, magenta stick, our structure; and an NNI having a phenylalanine scaffold, (orange stick) (26).

though this study did not explain how inhibitor binding would trigger these conformational changes, the results suggest that these inhibitors may act by causing a perturbation of the interaction between the fingertip  $\Lambda$ 1 loop and the thumb domain and simultaneously locking the enzyme in an opened

FIG. 4. Partial sequence alignment of representative HCV polymerase sequences from the most common genotypes: 1a, 1b (these structures), 2a, 2b, 2c, and 3a. Numbers to the left of the genotypes correspond to the accession numbers from GenBank™. Strictly conserved residues are shown in black on a pink background. Non-conserved residues are shown in red. A, alignment of residues displaced by the inhibitor. B, alignment of residues interacting with the inhibitor.

**A**

	20	21	22	23	24	25	26	27	28	29	30	31	32	33	34	35	36
AF011751_1a	K	L	P	I	N	A	L	S	N	S	L	L	R	H	H	N	L
AB016785_1b	K	L	P	I	N	A	L	S	N	S	L	L	R	H	H	N	M
AF177036_2a	K	L	P	I	N	P	L	S	N	S	L	L	R	Y	H	N	K
AF238486_2b	K	L	P	I	N	P	L	S	N	S	L	M	R	F	H	N	K
AB031663_2c	K	L	P	I	N	P	L	S	N	S	L	L	R	Y	H	N	K
AF046866_3a	K	L	P	I	S	P	L	S	N	S	L	L	R	H	H	N	L

**B**

	37	392	393	395	396	399	424	425	428	429	492	493	494	495	500	503
AF011751_1a	V	L	A	A	A	T	I	L	H	F	L	G	V	P	W	R
AB016785_1b	V	L	A	A	A	T	I	L	H	F	L	G	V	P	W	R
AF177036_2a	V	I	A	A	A	T	V	L	H	F	L	G	A	P	W	R
AF238486_2b	V	I	T	A	A	T	V	I	H	F	L	G	A	P	W	R
AB031663_2c	V	L	A	A	A	T	V	L	H	F	L	G	A	P	W	R
AF046866_3a	V	L	A	A	A	T	V	M	H	F	L	G	C	P	W	R

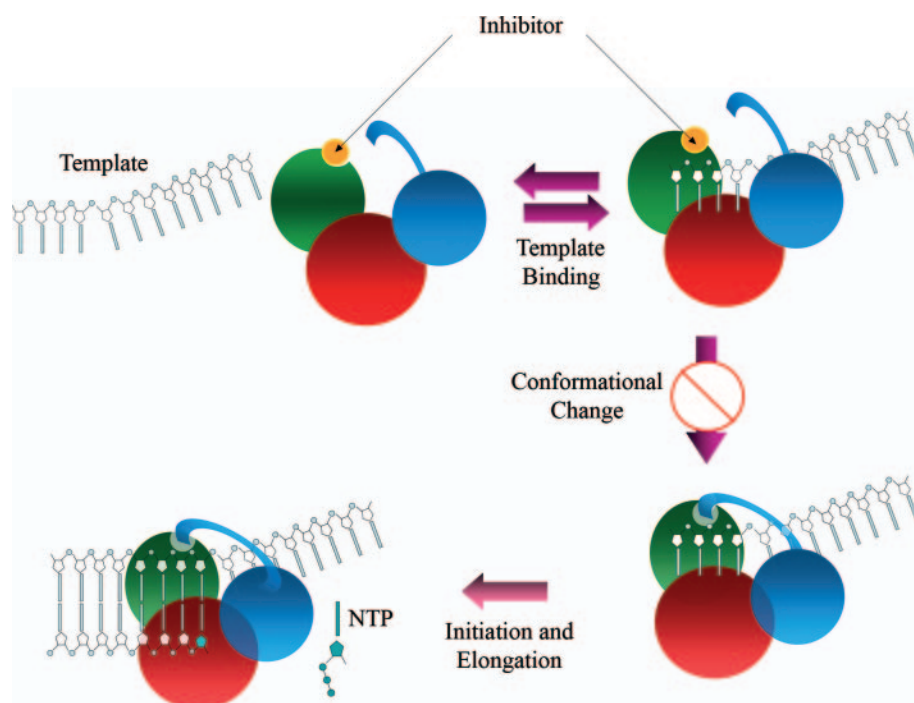


FIG. 5. Schematic mechanism of inhibition by indole-based compounds. The inhibitor is depicted as a yellow circle. The fingers, palm, and thumb domains are shown as spheres and colored as in Fig. 1A.

“inactive” conformation (22). Therefore, even if these two classes of NNIs bind to sites located in different regions of the thumb, they may ultimately inhibit the polymerase by a common mechanism.

**The Role of the Fingertip  $\alpha$ -Helix A**—The structures of the inhibited polymerase complexes reported here imply that in the apoenzyme the  $\Lambda 1$  loop is conformationally flexible allowing access of the indole-based inhibitors to the otherwise buried binding site. In the apostructure, the Leu-30 and Leu-31 side chains from  $\alpha$ -helix A only partially fill the pockets occupied by the inhibitor cyclohexyl and phenyl substituents, respectively (Fig. 2D). In fact, not only are the two side chains smaller than the two inhibitor cyclic substituents, but also, because of constraints imposed by the  $\alpha$ -helical structure in this region of the  $\Lambda 1$  loop, they protrude less deeply into the corresponding pockets. It is attractive to speculate that a suboptimal anchoring of fingers to the thumb established by  $\alpha$ -helix A might provide the polymerase with the conformational flexibility required during the different steps of RNA synthesis. The flexibility of the  $\Lambda 1$  loop and its role in holding the thumb and fingers together are

further supported by the recently solved structures of the polymerase genotype 2a (22) (see above).

The high sequence conservation among HCV genotypes of the region displaced by the inhibitor, as well as of residues forming the inhibitor binding pockets (Fig. 4), supports an essential function of  $\alpha$ -helix A-thumb domain interaction for NS5B activity. Consistently, mutation of Leu-30 to Ser or Arg results in an inactive enzyme (33). Helical regions at the tip of fingertip loops connecting the fingers and thumb are present in other viral RdRps (12–17, 19). The similarities in the structure and enzymatic mechanism (34) between NS5B and these polymerases suggest that flexibility of the fingertip loops could also be a feature of some of these RdRps, and inhibitor binding sites similar to the one described here could also be available for them.

**Conclusion**—Previous biochemical studies have suggested that the HCV polymerase catalyzes RNA synthesis through an ordered stepwise mechanism (24). The polymerase-RNA template complex is first formed rapidly. Second, a productive enzyme elongation complex is formed more slowly (24). The



indole-based inhibitors, similar to what has been observed for the structurally related benzimidazole-based inhibitors (24), bind and inhibit NS5B only prior to formation of the latter complex.<sup>3</sup>

Several pieces of evidence support our structure as a genuine model for the high affinity indole-based inhibitor polymerase interaction. First, the competition between these inhibitors and GTP and the lack of inhibitor binding of the point mutant P495L are in agreement with the structures here reported. Second, this class of inhibitors bind to the apoenzyme and to the initial template-enzyme complexes with similar affinities (24) suggesting that they bind similarly to both forms of the polymerase. Third, the almost perfect fit of the cyclohexyl and phenyl rings into the  $\alpha$ -helix A-derived binding site pockets is suggestive of a high affinity interaction. Fourth, although our inhibited structure revealed a rigid body rotation of the fingers relative to the palm and thumb domains, we did not observe any changes in the structure of the thumb domain itself. This suggests that the details of the interaction between thumb and inhibitor would be preserved even if in solution the polymerase adopted a more opened conformation when bound to the inhibitor.

When the published biochemical data are combined with the structures reported here, a model for the NS5B inhibition by the indole-based compounds can be proposed (Fig. 5). Before formation of a productive initiation complex, the fingertip  $\alpha$ -helix A is flexible and opens toward the solvent allowing binding of the inhibitor. After binding, the connection between the fingers and thumb domains is, at least partially, abrogated, and the  $\Lambda$ 1 loop can no longer mediate the concerted rearrangement of the polymerase domains needed for formation of a productive RNA-enzyme complex. Interestingly, when added after formation of the productive complex, the inhibitor did not bind or inhibit (24, 25) suggesting that during elongation either the binding site is not available because of a tighter interaction between the  $\Lambda$ 1 fingertip residues and thumb or because the polymerase has assumed a somewhat different shape.

In conclusion the structures reported here have identified a novel allosteric inhibitor binding site on the HCV NS5B polymerase that could not be predicted based on previous work and revealed the mechanism of inhibition of a new class of HCV NNIs. Moreover, the structures have shown the details of the interactions established by the inhibitor suggesting ways to improve the potency for this class of molecules. Finally, our study further supports a model whereby the polymerase  $\Lambda$ 1 loop regulates the coordinated movements of the fingers and thumb during the polymerase reaction cycle.

**Acknowledgments**—We thank the staff at the European Synchrotron Radiation Facility for assistance in the data collection, David Olsen, Alessandro Vannini, and Edwin Rydberg for useful discussions, and Emanuela Emili for help with the artwork.

<sup>3</sup> L. Tomei, unpublished results.

## REFERENCES

- Choo, Q. L., Kuo, G., Weiner, A. J., Overby, L. R., Bradley, D. W., and Houghton, M. (1989) *Science* **244**, 359–362
- Saito, I., Miyamura, T., Ohbayashi, A., Harada, H., Katayama, T., Kikuchi, S., Watanabe, Y., Koi, S., Onji, M., and Ohta, Y. (1990) *Proc. Natl. Acad. Sci. U. S. A.* **87**, 6547–6549
- Cohen, J. (1999) *Science* **285**, 26–30
- Zhong, W., Uss, A. S., Ferrari, E., Lau, J. Y., and Hong, Z. (2000) *J. Virol.* **74**, 2017–2022
- Ranjith-Kumar, C. T., Kim, Y. C., Gutshall, L., Silverman, C., Khandekar, S., Sarisky, R. T., and Kao, C. C. (2002) *J. Virol.* **76**, 12513–12525
- Shim, J. H., Larson, G., Wu, J. Z., and Hong, Z. (2002) *J. Virol.* **76**, 7030–7039
- Kao, C. C., Singh, P., and Ecker, D. J. (2001) *Virology* **287**, 251–260
- Ago, H., Adachi, T., Yoshida, A., Yamamoto, M., Habuka, N., Yatsunami, K., and Miyano, M. (1999) *Structure Fold. Des.* **7**, 1417–1426
- Bressanelli, S., Tomei, L., Roussel, A., Incitti, I., Vitale, R. L., Mathieu, M., De Francesco, R., and Rey, F. A. (1999) *Proc. Natl. Acad. Sci. U. S. A.* **96**, 13034–13039
- Lesburg, C. A., Cable, M. B., Ferrari, E., Hong, Z., Mannarino, A. F., and Weber, P. C. (1999) *Nat. Struct. Biol.* **6**, 937–943
- Ollis, D. L., Brick, P., Hamlin, R., Xuong, N. G., and Steitz, T. A. (1985) *Nature* **313**, 762–766
- Hansen, J. L., Long, A. M., and Schultz, S. C. (1997) *Structure (Camb.)* **5**, 1109–1122
- Thompson, A. A., and Peersen, O. B. (2004) *EMBO J.* **23**, 3462–3471
- Love, R. A., Maegley, K. A., Yu, X., Ferre, R. A., Lingardo, L. K., Diehl, W., Parge, H. E., Dragovich, P. S., and Fuhrman, S. A. (2004) *Structure (Camb.)* **12**, 1533–1544
- Appleby, T. C., Luecke, H., Shim, J. H., Wu, J. Z., Cheney, I. W., Zhong, W., Vogeley, L., Hong, Z., and Yao, N. (2005) *J. Virol.* **79**, 277–288
- Choi, K. H., Groarke, J. M., Young, D. C., Kuhn, R. J., Smith, J. L., Pevear, D. C., and Rossmann, M. G. (2004) *Proc. Natl. Acad. Sci. U. S. A.* **101**, 4425–4430
- Ng, K. K., Cherney, M. M., Vazquez, A. L., Machin, A., Alonso, J. M., Parra, F., and James, M. N. (2002) *J. Biol. Chem.* **277**, 1381–1387
- Tao, Y., Farsetta, D. L., Nibert, M. L., and Harrison, S. C. (2002) *Cell* **111**, 733–745
- Butcher, S. J., Grimes, J. M., Makeyev, E. V., Bamford, D. H., and Stuart, D. I. (2001) *Nature* **410**, 235–240
- O'Farrell, D., Trowbridge, R., Rowlands, D., and Jager, J. (2003) *J. Mol. Biol.* **326**, 1025–1035
- Bressanelli, S., Tomei, L., Rey, F. A., and De Francesco, R. (2002) *J. Virol.* **76**, 3482–3492
- Biswal, B. K., Cherney, M. M., Wang, M., Chan, L., Yannopoulos, C. G., Bilimoria, D., Nicolas, O., Bedard, J., and James, M. N. (2005) *J. Biol. Chem.* **280**, 18202–18210
- Love, R. A., Parge, H. E., Yu, X., Hickey, M. J., Diehl, W., Gao, J., Wriggers, H., Ekker, A., Wang, L., Thomson, J. A., Dragovich, P. S., and Fuhrman, S. A. (2003) *J. Virol.* **77**, 7575–7581
- Tomei, L., Altamura, S., Bartholomew, L., Biroccio, A., Ceccacci, A., Pacini, L., Narjes, F., Gennari, N., Bisbocci, M., Incitti, I., Orsatti, L., Harper, S., Stansfield, I., Rowley, M., De Francesco, R., and Migliaccio, G. (2003) *J. Virol.* **77**, 13225–13231
- McKercher, G., Beaulieu, P. L., Lamarre, D., LaPlante, S., Lefebvre, S., Pellerin, C., Thauvette, L., and Kukolj, G. (2004) *Nucleic Acids Res.* **32**, 422–431
- Wang, M., Ng, K. K., Cherney, M. M., Chan, L., Yannopoulos, C. G., Bedard, J., Morin, N., Nguyen-Ba, N., Alaoui-Ismaïli, M. H., Bethell, R. C., and James, M. N. (2003) *J. Biol. Chem.* **278**, 9489–9495
- Harper, S., Pacini, B., Avolio, S., Di Filippo, M., Migliaccio, G., Laufer, R., De Francesco, R., Rowley, M., and Narjes, F. (2005) *J. Med. Chem.* **48**, 1314–1317
- McHutchison, J. G., and Patel, K. (2002) *Hepatology* **36**, S245–252
- Tomei, L., Vitale, R. L., Incitti, I., Serafini, S., Altamura, S., Vitelli, A., and De Francesco, R. (2000) *J. Gen. Virol.* **81**, 759–767
- Tomei, L., Altamura, S., Bartholomew, L., Bisbocci, M., Bailey, C., Bosserman, M., Cellucci, A., Forte, E., Incitti, I., Orsatti, L., Koch, U., De Francesco, R., Olsen, D. B., Carroll, S. S., and Migliaccio, G. (2004) *J. Virol.* **78**, 938–946
- Collaborative Computational project, N. (1994) *Acta Crystallogr. Sect. D Biol. Crystallogr.* **50**, 760–763
- Laskowsky, R. A., MacArthur, M. W., Moss, D. S., and Thornton, J. M. (1993) *J. Appl. Crystallogr.* **26**, 283–291
- Labonte, P., Axelrod, V., Agarwal, A., Aulabaugh, A., Amin, A., and Mak, P. (2002) *J. Biol. Chem.* **277**, 38838–38846
- van Dijk, A. A., Makeyev, E. V., and Bamford, D. H. (2004) *J. Gen. Virol.* **85**, 1077–1093

**Interdomain Communication in Hepatitis C Virus Polymerase Abolished by Small Molecule Inhibitors Bound to a Novel Allosteric Site**

Stefania Di Marco, Cinzia Volpari, Licia Tomei, Sergio Altamura, Steven Harper, Frank Narjes, Uwe Koch, Michael Rowley, Raffaele De Francesco, Giovanni Migliaccio and Andrea Carfi

*J. Biol. Chem.* 2005, 280:29765-29770.

doi: 10.1074/jbc.M505423200 originally published online June 13, 2005

---

Access the most updated version of this article at doi: [10.1074/jbc.M505423200](https://doi.org/10.1074/jbc.M505423200)

Alerts:

- [When this article is cited](#)
- [When a correction for this article is posted](#)

[Click here](#) to choose from all of JBC's e-mail alerts

Supplemental material:

<http://www.jbc.org/content/suppl/2005/06/15/M505423200.DC1>

This article cites 34 references, 18 of which can be accessed free at

<http://www.jbc.org/content/280/33/29765.full.html#ref-list-1>